Comparative studies on regularization penalties for structural damage detection

Ziwei Luo and *†Ling Yu

MOE Key Laboratory of Disaster Forecast and Control in Engineering, School of Mechanics and Construction Engineering, Jinan University, Guangzhou, China.

*Presenting and †Corresponding author: lyu1997@163.com

Abstract

Structural damage detection (SDD) is an essential link to structural safety in the field of structural health monitoring (SHM). With the development of SHM technologies, higher requirements are necessary for the safety of structures. Therefore, many SDD methods have been emerging in the last decades. Due to the ill-posedness of SDD problems, regularization techniques are introduced to locate structural damages and quantify severities of damages with a higher accuracy. However, the influence of regularization penalties on SDD results is lack of consideration to date. In this study, based on the model updating technique, an intensive study is proposed to investigate the effect of different regularization penalties in structural damage patterns. First-order sensitivity analysis is chosen to establish the identified equation. Considering structural damage patterns, three regularization penalties, i.e. the l_2 norm, l_1 norm and $l_{1/2}$ norm penalties are adopted for this comparative study. The SDD problem is converted into a kind of optimization problems by defining an objective function with different regularization penalties, and they are finally solved by the particle swarm optimization (PSO) algorithm. The spring-mass model and cantilever beam are taken as examples in numerical simulations for comparative studies. The illustrated results show that there are significant effects on the SDD results using different regularization penalties. The l_2 norm penalty is more suitable for structural model updating. The l_1 norm penalty has positive effect on identifying structural damages for contiguous zones, and the $l_{1/2}$ norm penalty has higher accuracy for noncontiguous damage identification than the l_1 norm penalty, which provides a potential tool for SDD onsite in the SHM field.

Keywords: Structural health monitoring (SHM), structural damage detection (SDD), regularization, norm penalty, structural damage patterns, sensitivity analysis, particle swarm optimization (PSO).

Introduction

In recent years, more and more scholars have been devoting to ensure the safety of in-service structures [1]-[6]. As an effective way for monitoring long-term properties and states in the service life of structures, structural health monitoring (SHM) uses measured structural responses to estimate the change in structural states. Structural damage detection (SDD) is a vital step in the SHM field and is applied to locate and quantify damages of structures.

Modal-based method [1] is one kind of SDD methods to detect damages by modal parameters. The common modal parameters for SDD are frequencies and mode shapes. Effectively utilizing both frequencies and mode shapes for SDD has been proposed in many methods, and sensitivity analysis is a common technique to establish the identified equations in these methods. Cawley and Adams [2] proposed a SDD method using sensitivity analysis and frequencies. However, frequencies are global structural properties, and they are not sensitive to local damages. To overcome this shortcoming, mode shapes, local structural properties and so on, were introduced to the SDD method by Chen et al [3]. Li et al [4] improved SDD methods with the advantages of frequencies and mode shapes to improve accuracy of SDD results. However, accurate results are not obtained due to the ill-posedness of SDD problems.

Regularization techniques are common approaches to deal with the ill-posed problem. Many scholars have introduced regularization techniques into SDD. Tikhonov regularization method (referred to as l_2 norm regularization method) is a classical regularization technique, and has been used in some SDD studies. For example, Li and Law [5] presented an adaptive Tikhonov regularization method for solving the nonlinear model updating problem. SDD results obtained by the l_2 norm regularization method do not match the sparsity property of actual damages. Lasso regularization method (referred to as l_1 norm regularization method) based on modal updating techniques with natural frequencies and mode shapes was proposed by Hou et al. [6]. Moreover, the l_q ($0 < q < 1$) norm regularizations have been verified to obtain sparser solution than the l_1 norm regularization. The experimental study [7] has been conducted to show that the $l_{1/2}$ norm regularization can be taken as a representation among the l_q norm regularizations, and the $l_{1/2}$ norm regularization was introduced to SDD [8].

To compare performances of regularization techniques, Zhang and Xu [9] gave comparative studies between the l_2 norm and the l_1 norm regularization on damage detection. This study showed that the l_1 norm regularization exhibited superiority over the l_2 norm regularization for SDD. Sparsity of solutions and appropriate scenarios of regularization methods is diverse when different properties of norm penalties are used. Single damage pattern is unable to reflect effects of norm penalties, so more damage patterns will be considered in this paper.

On the other hand, swarm intelligence algorithms (SI) are evolutionary algorithms to promote the progress and development of scientific research. Due to their advantages of solving optimization problems, SI-based algorithms have been widely used in SDD, such as firefly algorithm [10], genetic algorithm [11], artificial bee colony algorithm [12] and so on. As one of SI-based algorithms, particle swarm optimization (PSO) was proposed by Kennedy and Eberhart [13] and widely applied in many fields due to its simplicity and easy implementation. PSO has been introduced into SDD for obtaining the optimal solutions [14]-[15].

In this study, comparative studies on SDD with different regularization methods are conducted. Sensitivity analysis is adopted to establish the relationship between structural damages and modal parameters. The l_2 norm penalty, the l_1 norm penalty and the $l_{1/2}$ norm penalty are selected to define objection functions respectively. The PSO algorithm is utilized to solve these objection functions. To compare the appropriate scenarios of regularization methods, a spring-mass model and a cantilever beam are simulated.

Theoretical background

Sensitivity Analysis

Structural frequencies and mode shapes are affected by the change in structural physical parameters. The sensitivity-based dynamic analysis method defines the first-order sensitivity analysis equation based on the correlation between structural modal parameters and physical parameters. It can detect damage locations and quantify damage severities based on finite element model and the sensitivity equation.

In this study, it is assumed that structural damages only cause the change in stiffness, and it is described by the change in elastic modulus. Thus, the global stiffness matrix of a *n*-element structure can be expressed as:

$$\mathbf{K} = \sum_{j=1}^{n} \alpha_j \mathbf{K}_j \left(0 \le \alpha_j \le 1\right) \tag{1}$$

where $\mathbf{K}_j$, α_j represent the *j*th element stiffness matrix and damage reduction factor, respectively.

The first-order sensitivity analysis equation based on derivatives of frequencies and mode shapes can be expressed as follows:

$$\begin{bmatrix} \frac{\partial \upsilon_1}{\partial \alpha_1} & \cdots & \frac{\partial \upsilon_1}{\partial \alpha_n} \\ \vdots & \ddots & \vdots \\ \frac{\partial \upsilon_m}{\partial \alpha_1} & \cdots & \frac{\partial \upsilon_m}{\partial \alpha_n} \\ \frac{\partial \boldsymbol{\varphi}_1}{\partial \alpha_1} & \cdots & \frac{\partial \boldsymbol{\varphi}_1}{\partial \alpha_n} \\ \vdots & \ddots & \vdots \\ \frac{\partial \boldsymbol{\varphi}_l}{\partial \alpha_1} & \cdots & \frac{\partial \boldsymbol{\varphi}_l}{\partial \alpha_n} \end{bmatrix} \boldsymbol{\Delta\alpha} = \mathbf{S}\boldsymbol{\Delta\alpha} \approx \mathbf{\Delta f} = \begin{Bmatrix} \mathbf{\Delta f}_\upsilon \\ \mathbf{\Delta f}_\varphi \end{Bmatrix} \tag{2}$$

where $\mathbf{\Delta f}_\upsilon = \{\Delta\upsilon_1, \Delta\upsilon_2, \ldots, \Delta\upsilon_m\}^T$ and $\mathbf{\Delta f}_\varphi = \{\boldsymbol{\Delta\varphi}_1, \boldsymbol{\Delta\varphi}_2, \ldots, \boldsymbol{\Delta\varphi}_l\}^T$ are the difference of frequencies and mode shapes, respectively. $\Delta\upsilon_p = \upsilon_{up} - \upsilon_{dp}$ ($p = 1, 2, \ldots, m$), υ_{up} and υ_{dp} are the *p*th frequencies in undamaged and damaged structures, respectively. *m* is the order of frequencies. $\boldsymbol{\Delta\varphi}_q = \boldsymbol{\varphi}_{uq} - \boldsymbol{\varphi}_{dq}$ ($q = 1, 2, \ldots, l$), $\boldsymbol{\varphi}_{uq}$ and $\boldsymbol{\varphi}_{dq}$ are the *p*th mode shapes in undamaged and damaged structures, respectively. *l* is the order of mode shapes. $\boldsymbol{\Delta\alpha} = \{\Delta\alpha_1, \Delta\alpha_2, \ldots, \Delta\alpha_n\}^T$ is the change in damage reduction factors. **S** is the first-order sensitivity matrix.

The least square method can be used to solve Eq. (2):

$$J_{\mathrm{LS}}(\boldsymbol{\Delta\alpha}) = \arg\min_{\boldsymbol{\Delta\alpha}} \frac{1}{2}\left\|\mathbf{S}\boldsymbol{\Delta\alpha} - \boldsymbol{\Delta}\mathbf{f}\right\|_2^2 \tag{3}$$

However, it cannot obtain a stable result for inverse problem due to the ill-conditioned matrix S and noise [16]. That is to say, due to the influence of noise, the solution of Eq. (2) is ill-posed. In this study, the influence of noise can be reduced and a stable solution can be obtained by combining sensitivity analysis with regularization methods.

Tikhonov Regularization

The principle of regularization methods is to replace the original ill-posed problem with an approximate well-posed problem whose solution equals original solution approximately. So Li and Law [5] introduced the l_2 norm regularization method into SDD for improving the identification precision. The l_2 norm regularization method [17] is a popular regularization method. It adds a quadratic penalty to Eq. (3):

$$J_2(\boldsymbol{\Delta\alpha}) = \arg\min_{\boldsymbol{\Delta\alpha}\in\mathbf{R}^P} \left\{\frac{1}{2}\left\|\mathbf{S}\boldsymbol{\Delta\alpha} - \boldsymbol{\Delta}\mathbf{f}\right\|_2^2 + \lambda\left\|\boldsymbol{\Delta\alpha}\right\|_2^2\right\} \tag{4}$$

where real solution and noise can be balanced by the regularization parameter ($\lambda > 0$). Regularization term controls the norm of solution. P is the dimension of $\boldsymbol{\Delta\alpha}$.

Sparse Regularization

The l_0 norm regularization method is an original definition of sparse regularization:

$$\arg\min_{\mathbf{X}} \left\{\frac{1}{2}\left\|\mathbf{X} - \mathbf{B}\right\|_2^2 + \lambda\left\|\mathbf{X}\right\|_0\right\} \tag{5}$$

where, $\left\|\mathbf{X}\right\|_0$ represents l_0 norm of vector $\mathbf{X}$.

The l_0 norm regularization method recovers sparse vector precisely, but it is a NP-hard problem. The l_1 norm regularization method, which was first proposed by Tibshirani [18] in 1996, can be used to approximately replace the l_0 norm regularization. The l_1 norm regularization method obtains sparse coefficient vector because coefficients with small absolute value will set to be zero:

$$\arg\min_{\mathbf{X}} \left\{\frac{1}{2}\left\|\mathbf{X} - \mathbf{B}\right\|_2^2 + \lambda\left\|\mathbf{X}\right\|_1\right\} \tag{6}$$

where, $\left\|\mathbf{X}\right\|_1$ represents l_1 norm of vector $\mathbf{X}$.

Eq. (6) can be solved by the soft-thresholding [19]:

$$\mathbf{X} = soft\left(\mathbf{B}, \lambda\right) = \begin{cases} \mathbf{B} + \lambda, & \mathbf{B} < -\lambda \\ 0, & \left|\mathbf{B}\right| \le \lambda \\ \mathbf{B} - \lambda, & \mathbf{B} > \lambda \end{cases} \tag{7}$$

To obtain sparser solution, the l_q norm regularizations were proposed after the l_1 norm regularization. Some studies focused on selecting the best value of q. They showed that the l_q norm regularizations gain sparser solutions as the q-value decreases. There are no significant different performances when $0 < q \leq 1/2$, so the $l_{1/2}$ norm regularization is a representative of the l_q norm regularizations [7]. The $l_{1/2}$ norm regularization method is more sparsity and viability than the l_1 norm regularization method, the $l_{1/2}$ norm regularization is defined as:

$$\arg\min_{\mathbf{X}} \left\{ \frac{1}{2} \left\| \mathbf{X} - \mathbf{B} \right\|_2^2 + \lambda \left\| \mathbf{X} \right\|_{1/2}^{1/2} \right\} \tag{8}$$

where, $\left\| \mathbf{X} \right\|_{1/2}$ represents $l_{1/2}$ norm of vector $\mathbf{X}$.

Compared with Eq. (6), a generalized shrinkage-thresholding operator [20] is given for the $l_{1/2}$ norm regularization:

$$\mathbf{X} = gsoft(\mathbf{B}, \lambda) = \begin{cases} 0, & |\mathbf{B}| \leq \tau^{GST}(\lambda) \\ \operatorname{sgn}(\mathbf{B}) s^{GST}(|\mathbf{B}|; \lambda) & |\mathbf{B}| > \tau^{GST}(\lambda) \end{cases} \tag{9}$$

where the thresholding τ^{GST} is given by:

$$\tau^{GST}(\lambda)\Big|_{q=\frac{1}{2}} = \left[2\lambda(1-q)\right]^{\frac{1}{2-q}} + \lambda q \left[2\lambda(1-q)\right]^{\frac{q-1}{2-q}} = \frac{3}{2}\lambda^{\frac{2}{3}} \tag{10}$$

and the $s^{GST}(|\mathbf{B}|;\lambda)$ can be calculated by the following formula:

$$s^{GST}(|\mathbf{B}|; \lambda) - \mathbf{B} + \frac{\lambda}{2}\left[s^{GST}(|\mathbf{B}|; \lambda)\right]^{-\frac{1}{2}} = 0 \tag{11}$$

For the SDD problem, structural damages occur in few locations, so the coefficient vector $\boldsymbol{\Delta\alpha}$ is a sparse vector. By respectively adding the l_1 norm and the $l_{1/2}$ norm regularization into Eq. (3), the following equations are obtained:

$$J_1(\boldsymbol{\Delta\alpha}) = \arg\min_{\boldsymbol{\Delta\alpha} \in \mathbf{R}^P} \left\{ \frac{1}{2} \left\| \mathbf{S}\boldsymbol{\Delta\alpha} - \boldsymbol{\Delta}\mathbf{f} \right\|_2^2 + \lambda \left\| \boldsymbol{\Delta\alpha} \right\|_1 \right\} \tag{12}$$

$$J_{1/2}(\boldsymbol{\Delta\alpha}) = \arg\min_{\boldsymbol{\Delta\alpha} \in \mathbf{R}^P} \left\{ \frac{1}{2} \left\| \mathbf{S}\boldsymbol{\Delta\alpha} - \boldsymbol{\Delta}\mathbf{f} \right\|_2^2 + \lambda \left\| \boldsymbol{\Delta\alpha} \right\|_{1/2}^{1/2} \right\} \tag{13}$$

Compared Eq. (12) with Eq. (6), it can be found that the objective functions in these two equations are different, so Eq. (12) cannot be directly solved by Eq. (6). Similarly, Eq. (13) cannot be directly solved by Eq. (7). To solve Eqs. (12) and (13), in this study, the PSO algorithm is introduced, by combining PSO algorithm with Eq. (6) and Eq. (7) respectively, the SDD results can be obtained by using Eqs. (12) and (13).

Particle Swarm Optimization

PSO is a heuristic algorithm, and it is inspired by group behavior of birds. With information sharing system of the bird flock, PSO simulates their foraging process in space. The solution process becomes orderly from unorderly, so an optimal solution can be obtained. PSO is simple and low computational cost compared to other novel heuristic algorithms. A solution of the optimization problem is a particle of search space. Velocity of each particle decides its direction and moving step. The best positions of individual particles $\mathbf{p}_{\mathrm{best}}$ and the previous best solution of the entire warm $\mathbf{g}_{\mathrm{best}}$ are used to update particle positions. That is to say, particles update their positions and velocities according to the following equations:

$$\mathbf{x}_j(t+1) = \mathbf{x}_j(t) + \mathbf{v}_j(t+1) \tag{14}$$

$$\mathbf{v}_j(t+1) = \mathbf{v}_j(t) + c_1 \cdot r_1 \cdot \left(\mathbf{p}_{best_j}(t) - \mathbf{x}_j(t)\right) + c_2 \cdot r_2 \cdot \left(\mathbf{g}_{best_j}(t) - \mathbf{x}_j(t)\right) \tag{15}$$

where $\mathbf{x}_j$ and $\mathbf{v}_j$ are the position and velocity of the jth particle, respectively. t is the iterative number. r_1 and r_2 are uniformly distributed random numbers in the range of [0,1], and the cognitive coefficient c_1 and the social coefficient c_2 are equal to 2.

In this study, Eqs. (4), (12) and (13) are optimization problems, so they can be solved by PSO. To obtain accurate solutions and reduce computation time, Eqs. (7) and (9) are added into each particle to solve Eqs. (12) and (13), respectively.

Numerical Simulations

To compare the appropriate scenarios of different regularization methods, a 2-DOF spring-mass model and a cantilever beam with the dimension of 0.7 m×0.05 m×0.01 m are adopted to simulate damages.

Spring-mass model

A 2-DOF spring-mass model is shown in Fig. 1. The stiffness and the mass of each DOF are 150 kN/m and 100 kg, respectively. The first two frequencies of the structure are 3.8096Hz and 9.9736Hz, respectively.

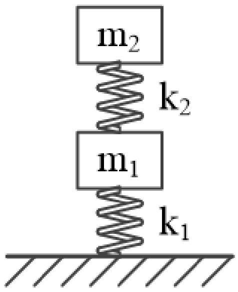

Figure 1. Spring-mass model

Gaussian white noise is the ideal model for analyzing additive noise in channels, so it is used to discuss the effect of noise on SDD results. In this study, measurement noise is considered to be related to the change in frequencies and mode shapes. Frequencies and mode shapes with noise are defined as follows:

$$\upsilon_i = \upsilon_i^{\,a} + \varepsilon_\upsilon R_i \left(\frac{\left\|\boldsymbol{\upsilon}_s - \boldsymbol{\upsilon}_e\right\|_2}{m}\right) \tag{16}$$

$$\varphi_{ij} = \varphi_{ij}^{\,a} + \varepsilon_\varphi R_{ij} \left(\frac{\left\|\boldsymbol{\varphi}_s - \boldsymbol{\varphi}_e\right\|_2}{lN}\right) \tag{17}$$

where, υ_i^a and υ_i (i = 1, 2, …, m) are the ith frequency and the one with noise, respectively. φ_{ij}^a and φ_{ij} (i = 1, 2, …, l; j = 1, 2, …, N) are the jth element of the ith mode shape and the one with noise, respectively. N is the length of each mode shape vector. $\boldsymbol{\upsilon}_s$ and $\boldsymbol{\upsilon}_e$ are vectors of frequencies in undamaged and damaged structures, respectively. $\boldsymbol{\varphi}_s$ and $\boldsymbol{\varphi}_e$ are rearranged vectors of mode shapes in undamaged and damaged structures, respectively. ε_υ and ε_φ are noise levels of frequencies and mode shapes, respectively. R_i and R_{ij} are random numbers subjected to the standard normal distribution.

As shown in Table 1, four damage scenarios are considered to compare properties of the l_2 norm regularization, the l_1 norm regularization and the $l_{1/2}$ norm regularization. Sketch maps of cost functions and norm penalties are offered to illustrate the appropriate scenarios of different regularization methods.

The SDD results are shown in Figs. 2-7. Where, (a) represents a sketch map of cost functions and norm penalties under different scenarios. The blue lines are constant value lines of cost functions and their radii are same in Figs. 2-3. The green lines are constant value lines of norm penalties and their junctions of coordinating axis are same in Figs. 4-6. The black points are possible values of actual $\boldsymbol{\Delta\alpha}$ with noise and the black dotted lines are possible constant value lines of cost functions.

Table 1. Damage scenarios for spring-mass model

Scenario no.	Damage degrees @ damaged elements	Noise levels	Values of m and l	Norm penalties	λ	Predicted damage numbers
1	10%@E1, 8%@E2	0%	m=l=2	l_2	0.0040	2
				l_1	0.0273	
				$l_{1/2}$	0.1000	
2	10%@E1, 2%@E2	0%	m=l=2	$l_{1/2}$	0.4300	1
3	10%@E2	1%	m=2, l=0	l_2	0.0017	2
				l_1	30	1
				$l_{1/2}$	859.1	1
4	10%@E2	10%	m=2, l=0	l_1	11.1970	2

Same SDD results can be identified when each DOF is damaged, as shown in Fig. 2. To analyze properties of norm penalties, the radii of cost functions are kept same and their regularization parameters are different. It shows that the l_2 norm regularization, the l_1 norm regularization and the $l_{1/2}$ norm regularization can detect multiple damages in scenario 1.

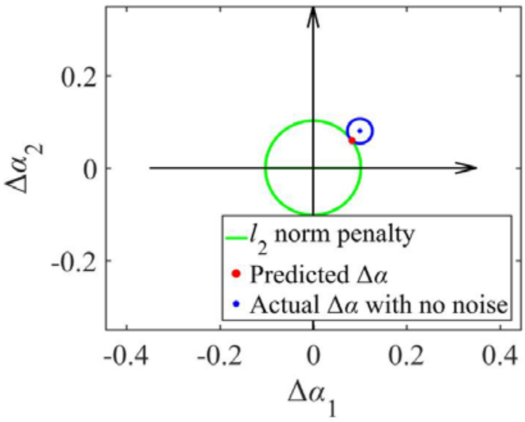

(a) Sketch map by adding l_2 norm penalty

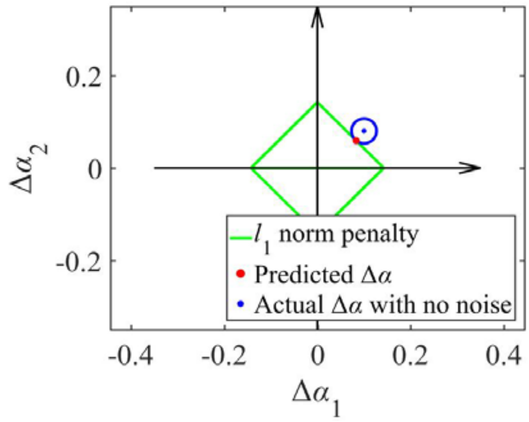

(b) Sketch map by adding l_1 norm penalty

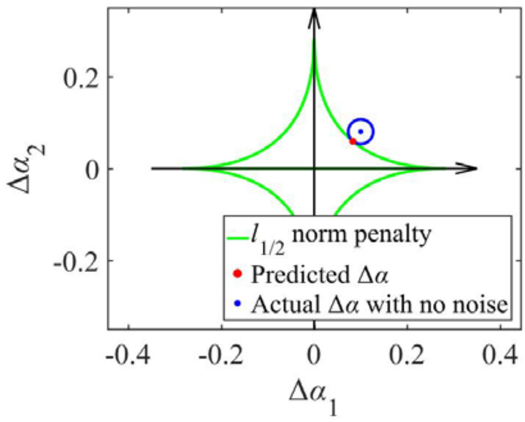

(c) Sketch map by adding $l_{1/2}$ norm penalty

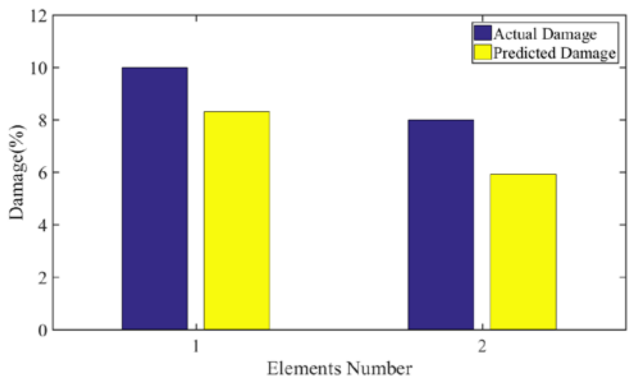

(d) Identified damage results

Figure 2. SDD results for spring-mass model in scenario 1

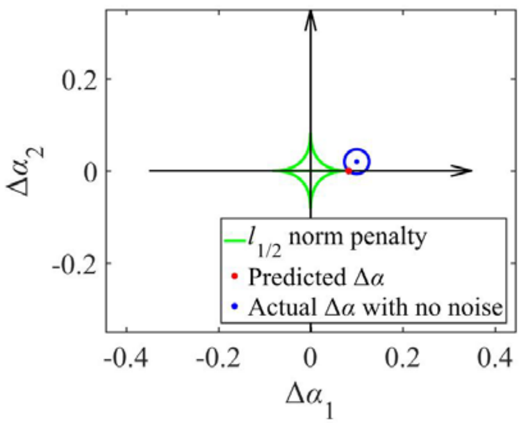

(a) Sketch map

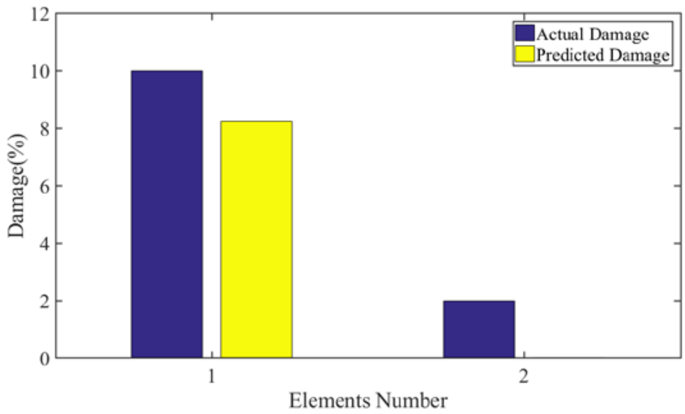

(b) Identified damage results

Figure 3. SDD results for spring-mass model in scenario 2 by adding $l_{1/2}$ norm penalty

By adding the $l_{1/2}$ norm penalty, the SDD result in scenario 1 are compared with that in scenario 2. Different damage degrees lead to different identified results of damage locations even if same damage locations are assumed. In scenario 2, great difference of damage degrees between element 1 and element 2 is given, and the $l_{1/2}$ norm penalty makes the SDD results sparse. Distinct from the sketch maps in Figs. 2(c) and 3(a), the cost function and the $l_{1/2}$ norm penalty intersect at coordinate axis. This is the reason why single damage is identified in scenario 2.

In scenario 3, multiple damages are identified when the l_2 norm penalty is added in the objective function, but one damage is identified when other two norm regularizations are used. Due to the influence of noise, the identified result $\boldsymbol{\Delta\alpha}$ will go away from the coordinate axis without adding penalty. Therefore, when the penalty is added, the junction between the contour lines of cost functions and the l_2 norm penalty is not on the axis. Under these circumstances, sparse solution cannot be obtained by adding the l_2 norm regularization.

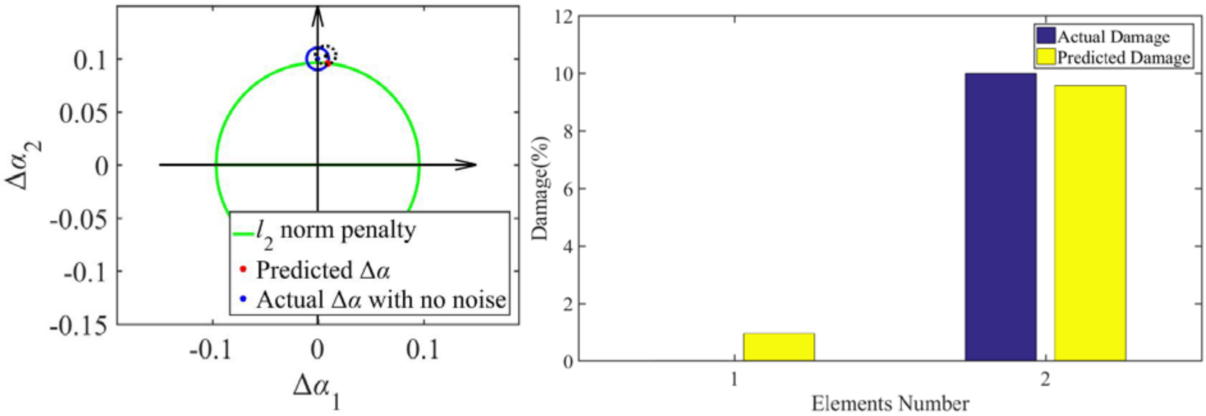

(a) Sketch map (b) Identified damage results

Figure 4. SDD results for spring-mass model in scenario 3 by adding l_2 norm penalty

SDD results are similar in scenario 3 when the l_1 norm and the $l_{1/2}$ norm penalty are respectively used. Different norm penalties give different spaces for the objective functions. Sparse solutions can be obtained due to the angles of the l_1 norm and $l_{1/2}$ norm penalties, which is different from the l_2 norm penalty. As a result, horned spaces of norm penalties are more beneficial to obtain sparse results. On the other hand, Figs. 2(a) and 4(a) shows that dense results are easy to be obtained by using the l_2 norm regularization.

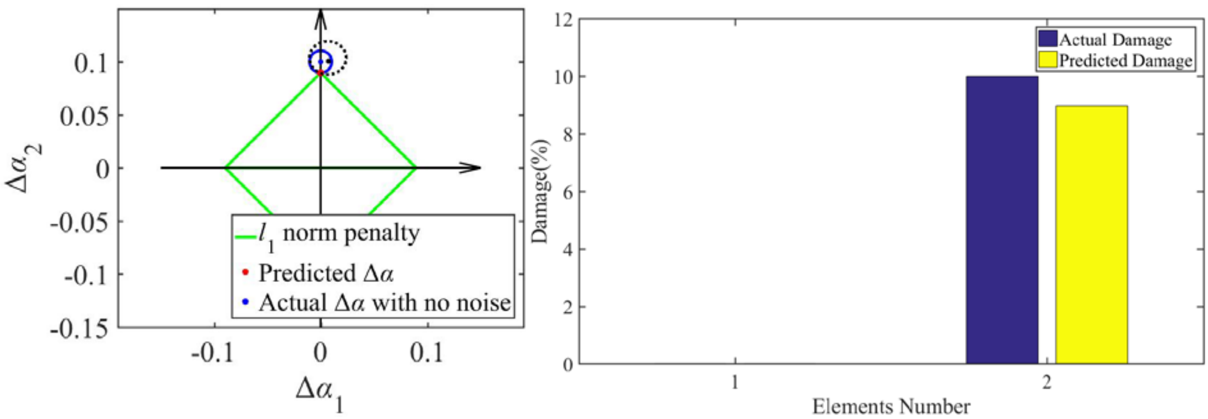

(a) Sketch map (b) Identified damage results

Figure 5. SDD results for spring-mass model in scenario 3 by adding l_1 norm penalty

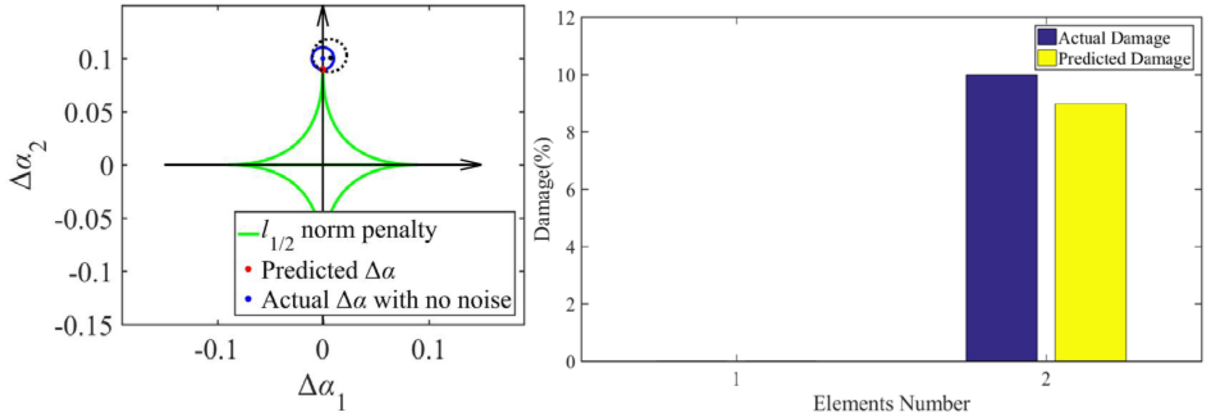

(a) Sketch map (b) Identified damage results

Figure 6. SDD results for spring-mass model in scenario 3 by adding $l_{1/2}$ norm penalty

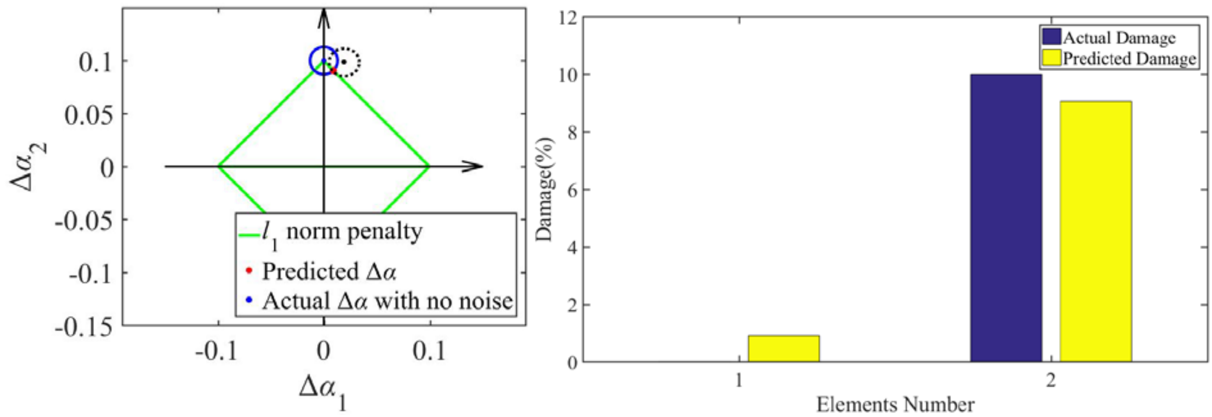

(a) Sketch map (b) Identified damage results

Figure 7. SDD results for spring-mass model in scenario 4 by adding l_1 norm penalty

Compared Figs. 5 and 7, it shows that the l_1 norm regularization does not obtain a sparse solution when the noise level increases, and great biases is produced due to the influence of noise. The junction between the contour lines of cost functions and the l_1 norm penalties is not on the axis. It indicates that both dense and sparse results may be identified by using the l_1 norm regularization.

By comparing Figs. 3, 5, 6 and 7, it shows that the curvatures of norm penalties will affect the SDD results. The sharp change in curvature increases the availability of getting sparse results. Thus, the $l_{1/2}$ norm regularization is more suitable for application in detecting sparse damages.

Some brief conclusions are summarized as follows: firstly, the l_2 norm regularization easily obtains a dense result, so it may have a good performance in the application of model updating. Secondly, dense or sparse solutions may be identified by the l_1 norm regularization, so it is more suitable to detect contiguous damages than the $l_{1/2}$ norm regularization. Thirdly, the $l_{1/2}$ norm regularization gets sparser results with a high probability than the l_1 norm regularization, so it is suitable for detecting noncontiguous damages.

Cantilever beam

To select appropriate regularization methods for different problems, a cantilever beam is simulated. As shown in Fig. 8, the cantilever beam is divided into ten elements. Numbers in circles represent element numbers. The elastic modulus is 2.01×10^{11} N/m^2 and the density is 7800 kg/m^3 for each element.

As shown in Table 2, seven damage scenarios are considered to select appropriate regularization methods for different scenarios. Four structural damage patterns, i.e. model updating, contiguous damages, noncontiguous damages and composite damages are offered to distinguish properties of different regularization methods. SDD results are shown in Figs. 9-15.

Table 2. Damage scenarios for cantilever beam

Scenario no.	Damage degrees @ damaged elements	Noise levels	Values of m and l	Norm penalties	λ	Damage patterns
1	3%@E1-E10	15%	m=l=9	l_2 l_1 $l_{1/2}$	0.3	model updating
2	0.8%@E1, E9 0.9%@E3, E5 1.1%@E4, E8 1%@E2, E6, E7, E10	10%		l_2 l_1 $l_{1/2}$	0.2	
3	5%@E4, 13%@E5 7%@E6	15%		l_2 l_1 $l_{1/2}$	0.15	contiguous damages
4	6%@E7, 4%@E8 8%@E9	10%		l_2 l_1 $l_{1/2}$	0.2	
5	12%@E2, 6%@E4 10%@E6	15%		l_2 l_1 $l_{1/2}$	0.09	noncontiguous damages
6	5%@E3, 10%@E5 7%@E9	10%		l_2 l_1 $l_{1/2}$	0.09	
7	10%@E4, 5%@E7 14%@E8, 6%@E9	15%		l_2 l_1 $l_{1/2}$	0.16	composite damages

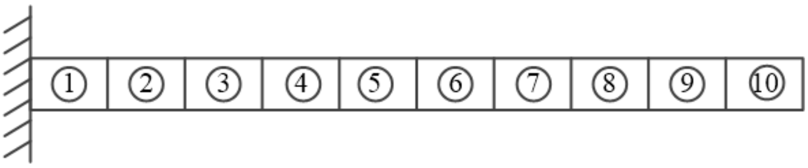

Figure 8. 10-element cantilever beam

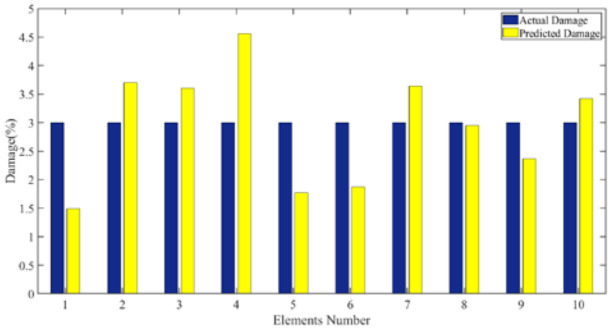

(a)

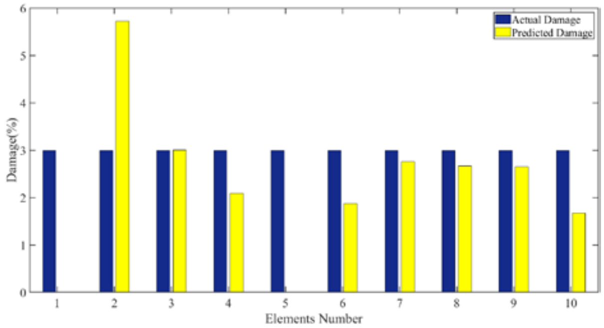

(b)

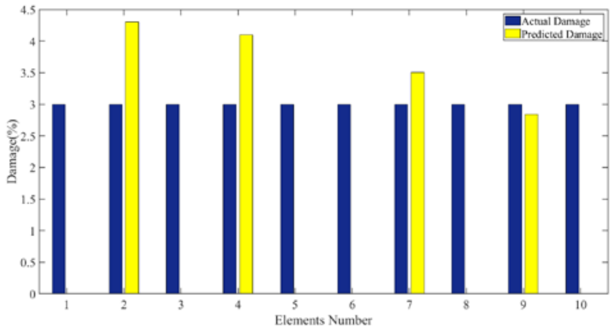

(c)

Figure 9. SDD results for cantilever beam in scenario 1 by adding different norm penalties: (a) l_2 norm penalty (b) l_1 norm penalty (c) $l_{1/2}$ norm penalty

In scenarios 1 and 2, dense results are obtained when the l_2 norm penalty is added into the objection functions, and sparse results are obtained by other regularization methods. Moreover, the solution by adding the $l_{1/2}$ norm regularization is sparser than that by adding the l_1 norm regularization. It can be concluded that the l_2 norm regularization is more suitable for application in model updating.

As mentioned above, the l_1 norm regularization is able to detect sparse and dense damages. It has good performances in scenarios 3 and 4. Damage locations can be effectively identified and quantify the damage degrees. The $l_{1/2}$ norm regularization can only detect two damage locations with a lower precision in these scenarios. It shows that the l_1 norm regularization has the ability to identify contiguous damages.

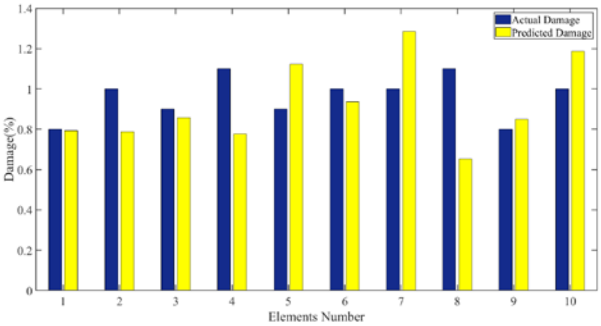

(a)

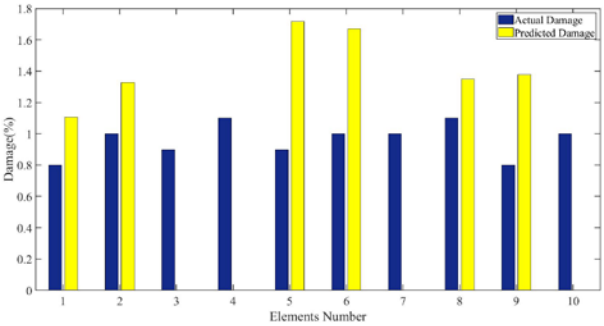

(b)

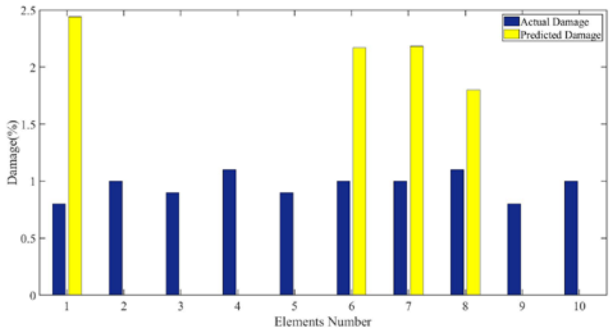

(c)

Figure 10. SDD results for cantilever beam in scenario 2 by adding different norm penalties: (a) l_2 norm penalty (b) l_1 norm penalty (c) $l_{1/2}$ norm penalty

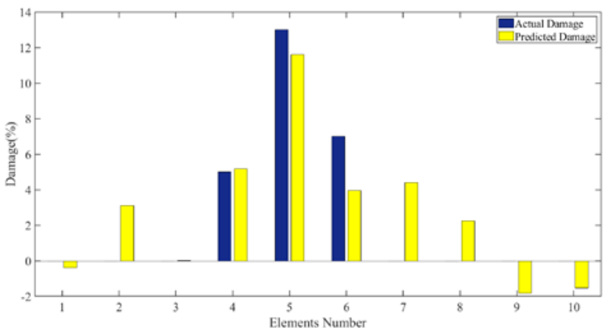

(a)

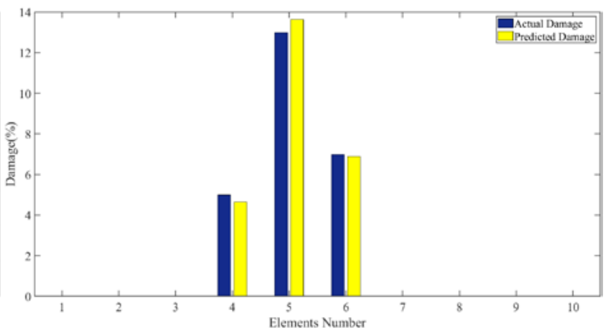

(b)

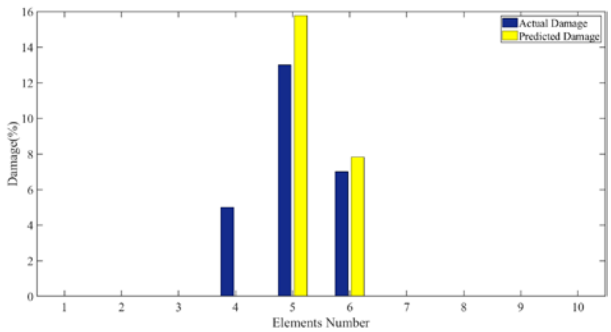

(c)

Figure 11. SDD results for cantilever beam in scenario 3 by adding different norm penalties: (a) l_2 norm penalty (b) l_1 norm penalty (c) $l_{1/2}$ norm penalty

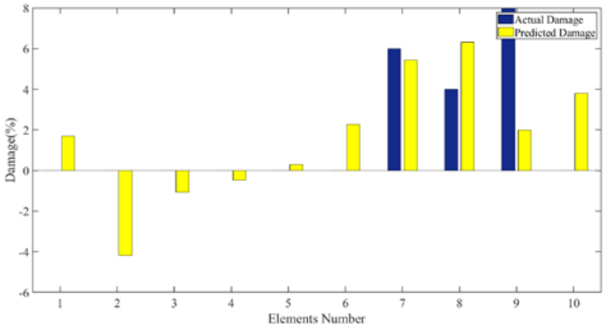

(a)

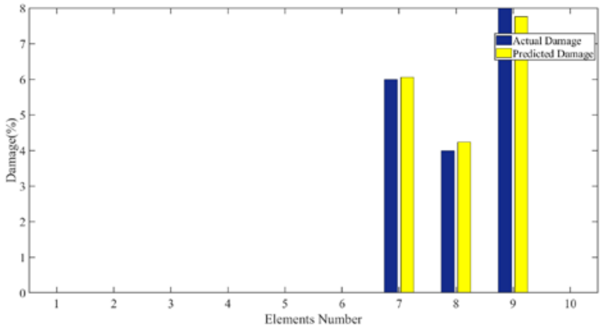

(b)

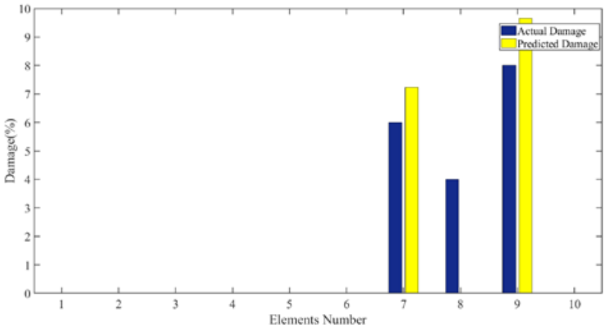

(c)

Figure 12. SDD results for cantilever beam in scenario 4 by adding different norm penalties: (a) l_2 norm penalty (b) l_1 norm penalty (c) $l_{1/2}$ norm penalty

Different from first two scenarios, exact damage results can be identified by adding the $l_{1/2}$ norm penalty to objection functions in scenarios 5 and 6. As indicated in the second conclusion, the l_1 norm regularization can identify contiguous damages. It may lead to misjudging near the actual damages. In this pattern of scenarios, the $l_{1/2}$ norm regularization can make good use of its advantage which makes the solution sparser. It is suitable for detecting noncontiguous damages.

For contiguous and noncontiguous damages, the l_2 norm regularization performs badly to detect them. Damage locations are misjudged in scenarios 3-7. The l_2 norm penalty is different from the l_1 norm and $l_{1/2}$ norm penalties. In the solving process, each element of the solution is not equal to zero by using the l_2 norm regularization. So the l_2 norm regularization is unreasonable for detecting sparse damages.

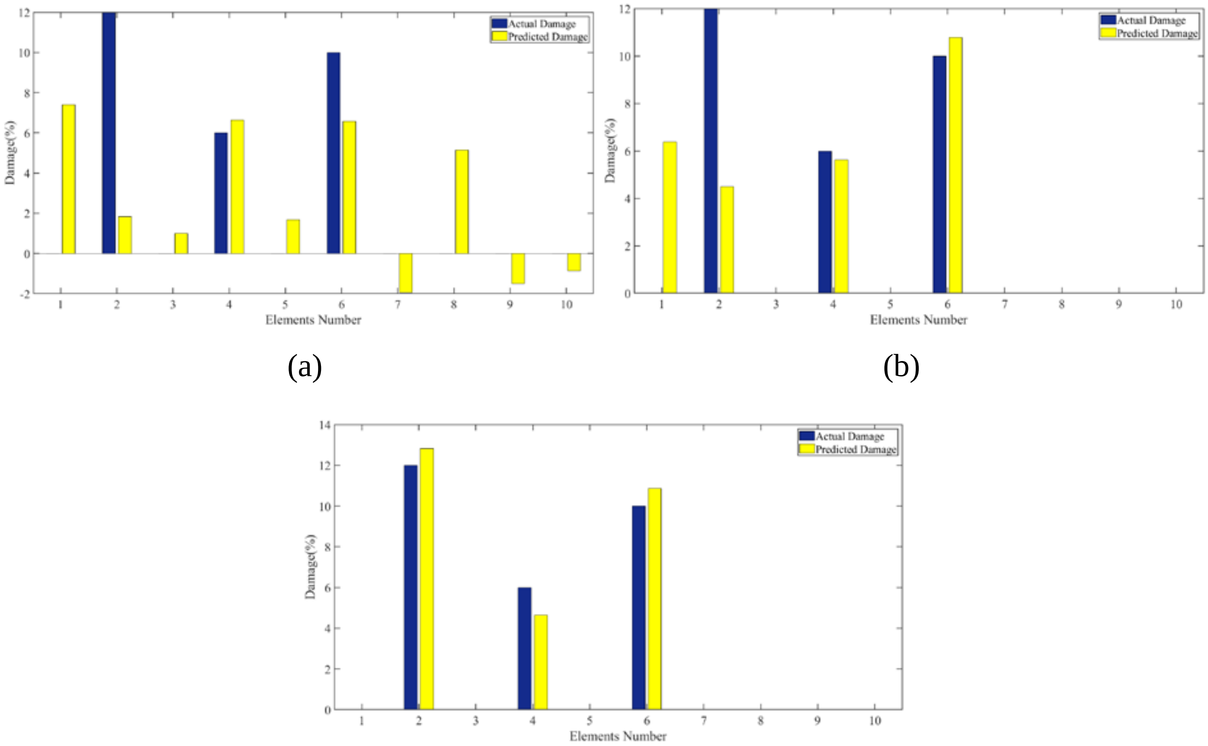

(a) (b)

(c)

Figure 13. SDD results for cantilever beam in scenario 5 by adding different norm penalties: (a) l_2 norm penalty (b) l_1 norm penalty (c) $l_{1/2}$ norm penalty

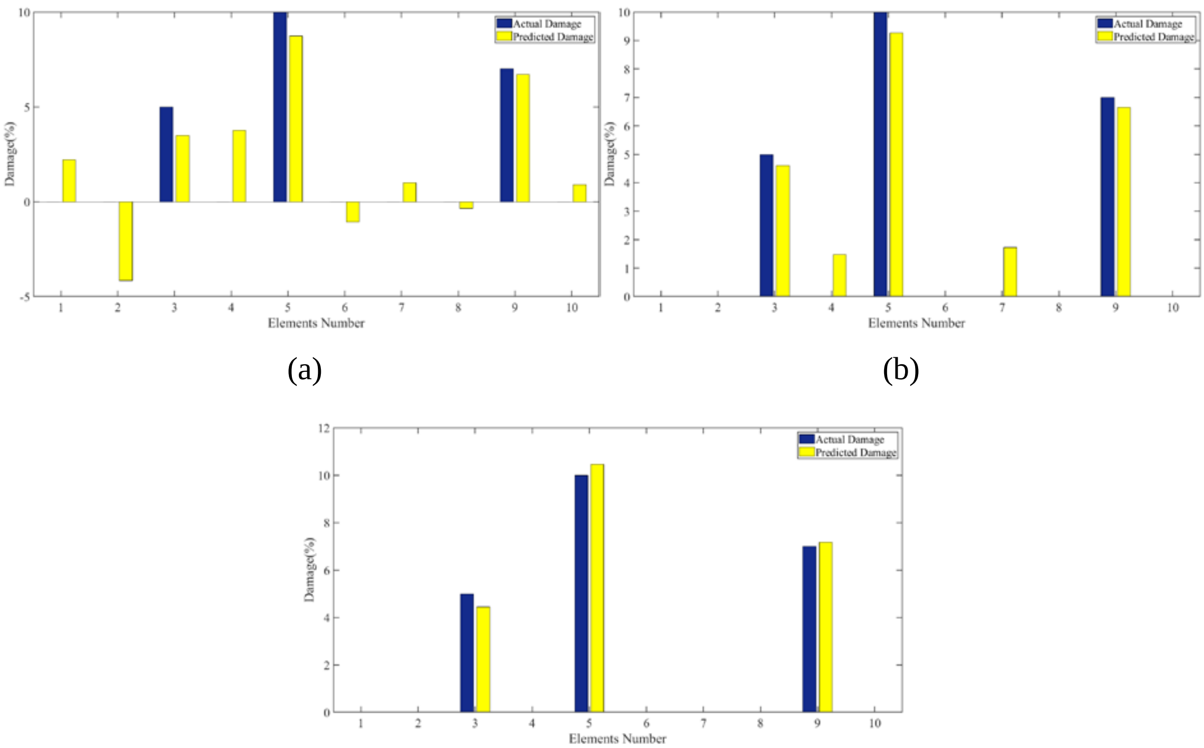

(a) (b)

(c)

Figure 14. SDD results for cantilever beam in scenario 6 by adding different norm penalties: (a) l_2 norm penalty (b) l_1 norm penalty (c) $l_{1/2}$ norm penalty

Combining contiguous and noncontiguous damages, composite damages are set in scenario 7. SDD results by adding the l_1 norm penalty are more accurate than ones by adding the $l_{1/2}$ norm penalty, but it does not mean that the l_1 norm regularization is always able to obtain good results for composite damages, because only one damage location is not detected by the $l_{1/2}$ norm regularization. More future work should be done to verify their abilities in the further studies.

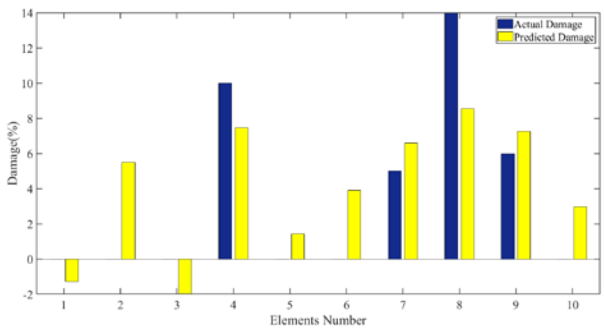

(a)

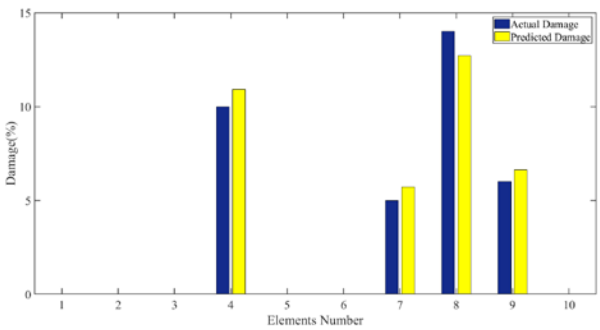

(b)

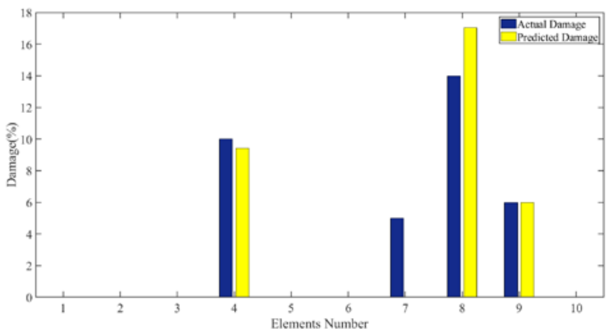

(c)

Figure 15. SDD results for cantilever beam in scenario 7 by adding different norm penalties: (a) l_2 norm penalty (b) l_1 norm penalty (c) $l_{1/2}$ norm penalty

Conclusions

In this study, based on sensitivity analysis method, different norm regularization methods, i.e. l_2 norm, l_1 norm and $l_{1/2}$ norm penalties, are compared to distinguish their abilities of detecting structural damages. Objective functions are defined by adding different norm penalties, and these functions are solved by the particle swarm optimization (PSO). A 2-DOF spring-mass model and a cantilever beam are simulated to analyze properties of the l_2 norm regularization, the l_1 norm regularization and the $l_{1/2}$ norm regularization, respectively. Sketch maps of cost functions and norm penalties under different scenarios are drawn to describe their relationship with predicted solution intuitively. Due to different application scopes, diverse damage scenarios are given in two numerical simulation models. Some main conclusions can be made as follows:

1) Dense solutions can be obtained when l_2 norm penalty is used, so the l_2 norm

regularization has a good performance in the application of model updating.

2) Dense solutions or sparse solutions can be identified by the l_1 norm regularization which depends on the deviation of actual solution from the coordinate axis. Sparse results can be obtained when the deviation is small. Otherwise, dense results will be obtained. So the l_1 norm regularization has ability to detect contiguous damages.
3) A dense result will be obtained due to the influence of noise. The $l_{1/2}$ norm regularization can address this issue effectively. Comparing with the l_1 norm regularization, the $l_{1/2}$ norm regularization can obtain sparser solution, and it is suitable for detecting noncontiguous damages.

Acknowledgments

The project is jointly supported by the National Natural Science Foundation of China with Grant Numbers 51678278 and 51278226.

References

[1] Das, S., Saha, P. and Patro, S. K. (2016) Vibration-based damage detection techniques used for health monitoring of structures: a review, *Journal of Civil Structural Health Monitoring* **6**, 477-507.
[2] Cawley, P. and Adams, R. D. (1979) The location of defects in structures from measurements of natural frequencies, *Journal of Strain Analysis* **14**, 49-57.
[3] Chen, J. C. and Garba, J. A. (1988) On-orbit damage assessment for large space structures, *AIAA Journal* **26**, 1119-1126.
[4] Li, H., Huang, Y., Ou, J. and Bao, Y. (2011) Fractal dimension-based damage detection method for beams with a uniform cross-section, *Computer-Aided Civil and Infrastructure Engineering* **26**, 190-206.
[5] Li, X. Y. and Law, S. S. (2010) Adaptive Tikhonov regularization for damage detection based on nonlinear model updating, *Mechanical Systems and Signal Processing* **24**, 1646-1664.
[6] Hou, R., Xia, Y. and Zhou, X. (2017) Structural damage detection based on l_1 regularization using natural frequencies and mode shapes, *Structural Control and Health Monitoring* **25**, e2107.
[7] Xu, Z. B., Guo, H. L., Wang, Y. and Zhang, H. (2012) Representative of $L_{1/2}$ regularization among L_q ($0 < q \leq 1$) regularizations: an experimental study based on phase diagram, *Acta Automatica Sinica* **38**, 1225-1228.
[8] Luo, Z. W. and Yu, L., PSO-based sparse regularization approach for structural damage detection, *2017 13th International Conference on Natural Computation, Fuzzy Systems and Knowledge Discovery (ICNC-FSKD)*, Yong, L., Liang, Z., Guoyong, C., Guoqing, X., Kenli, L. and Lipo, W., Eds., Guilin, China, 2017, 1034-1040.
[9] Zhang, C. D. and Xu, Y. L. (2015) Comparative studies on damage identification with Tikhonov regularization and sparse regularization, *Structural Control and Health Monitoring* **23**, 560-579.
[10] Pan, C. D. and Yu, L. (2014) Moving force identification based on firefly algorithm, *Advanced Materials Research* **919-921**, 329-333.
[11] Ullah, I., Sinha, J. K. and Pinkerton, A. (2013) Vibration-based delamination detection in a composite plate, *Mechanics of Advanced Materials and Structures* **20**, 536-551.
[12] Ding, Z. H., Huang, M. and Lu, Z. R. (2016) Structural damage detection using artificial bee colony algorithm with hybrid search strategy, *Swarm and Evolutionary Computation* **28**, 1-13.
[13] Kennedy, J. and Everhart, R. (2002) Particle swarm optimization, *Int Conf Neural Netw* **4**, 1942-1948.
[14] Wei, Z., Liu, J. and Lu, Z. (2017) Structural damage detection using improved particle swarm optimization, *Inverse Problems in Science and Engineering* **26**, 792-810.
[15] Gokdag, H. and Yildiz, A. R. (2012) Structural damage detection using modal parameters and particle swarm optimization, *Materials Testing* **54**, 416-420.
[16] Hansen, P. C., Nagy, J. G. and O'leary, D. P. (2006) *Deblurring images: matrices, spectra, and filtering*, Society for Industrial and Applied Mathematics, USA.
[17] Tikhonov, A. N. and Arsenin, V. Y. (1977) *Methods for solving ill-posed problems*, John Wiley and Sons, USA.
[18] Tibshirani, R. (1996) Regression shrinkage and selection via the lasso, *Journal of the Royal Statistical Society: Series B (Methodological)* **58**, 267-288.
[19] Selesnick, I. W. (2010) Sparse signal restoration, *Polytech-nic Uni*, 1-16.
[20] Zuo, W., Ren, D., Zhang, D., Gu, S. and Zhang, L. (2016) Learning iteration-wise generalized shrinkage-thresholding operators for blind deconvolution, *IEEE Transactions on Image Processing* **25**, 1751-1764.